Dye Sensitized Solar Cells based on Titania Nanomaterials

F. N. Castellano

Center for Photochemical Sciences
BOWLING GREEN STATE UNIVERSITY
LIGHTING THE WAY

Metal Oxide Dye Sensitized Solar Cells

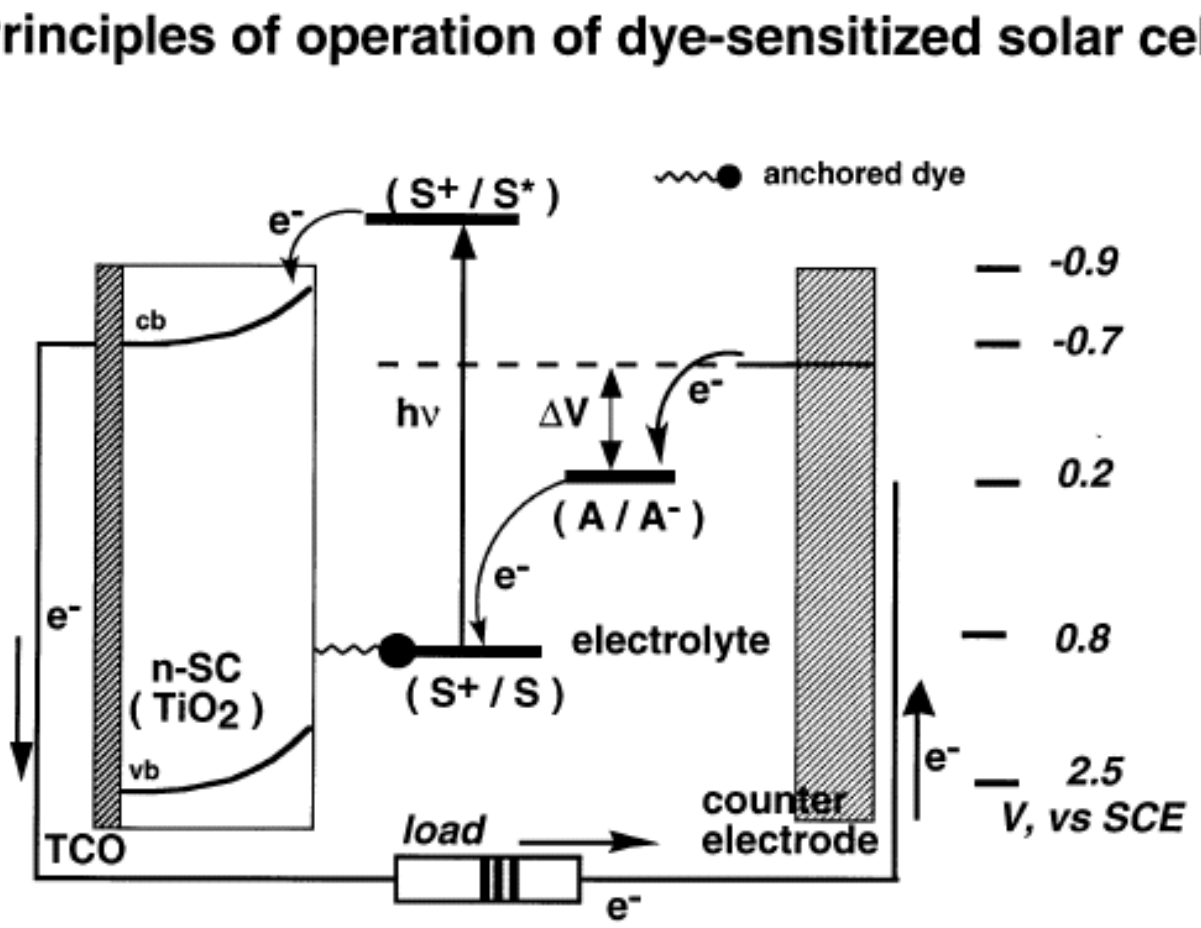

K. Kalyanasundaram & M. Gratzel *Coord. Chem. Rev.* **1998**, *177*, 347-414

Another Cartoon

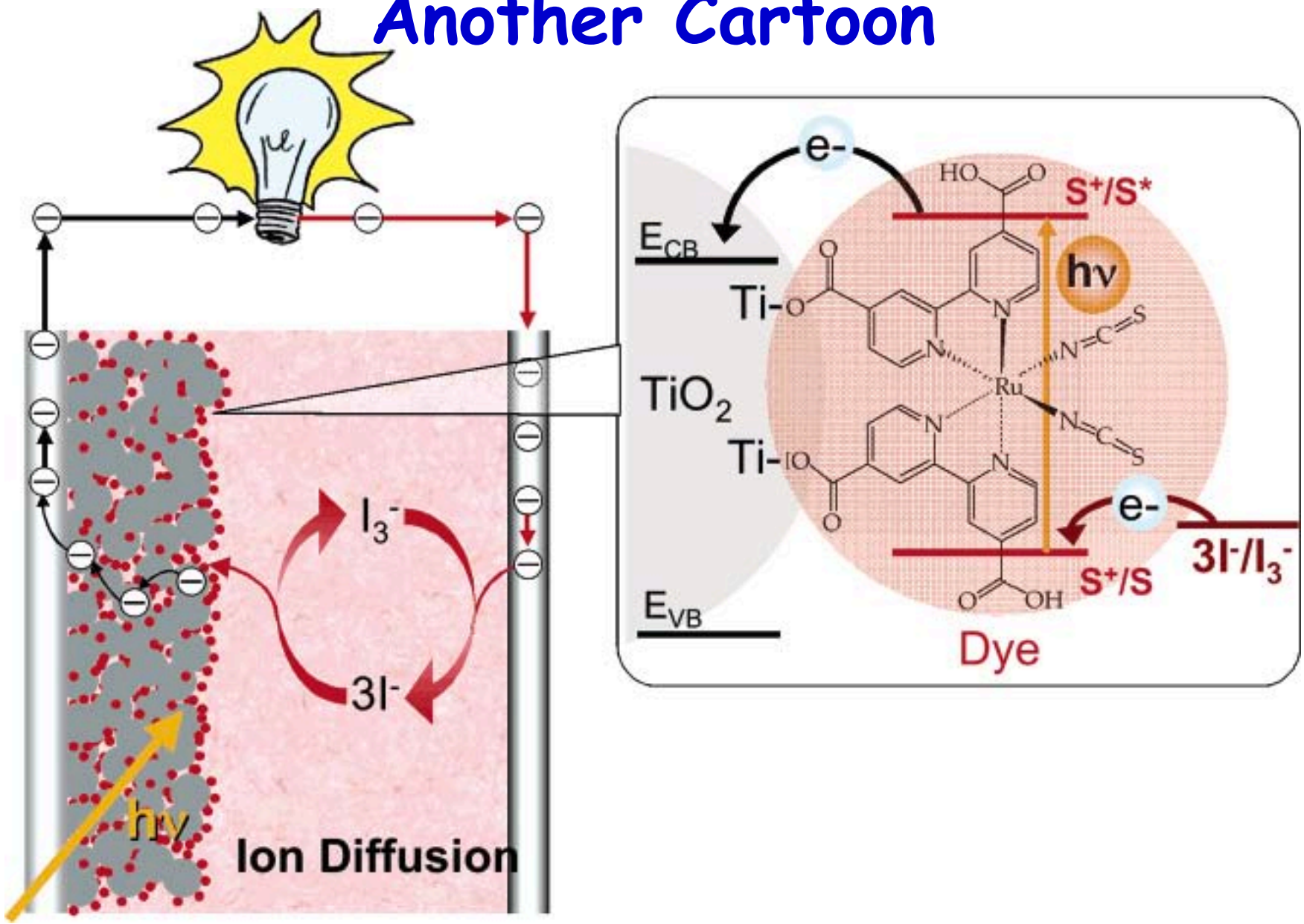

…Yet Another Cartoon

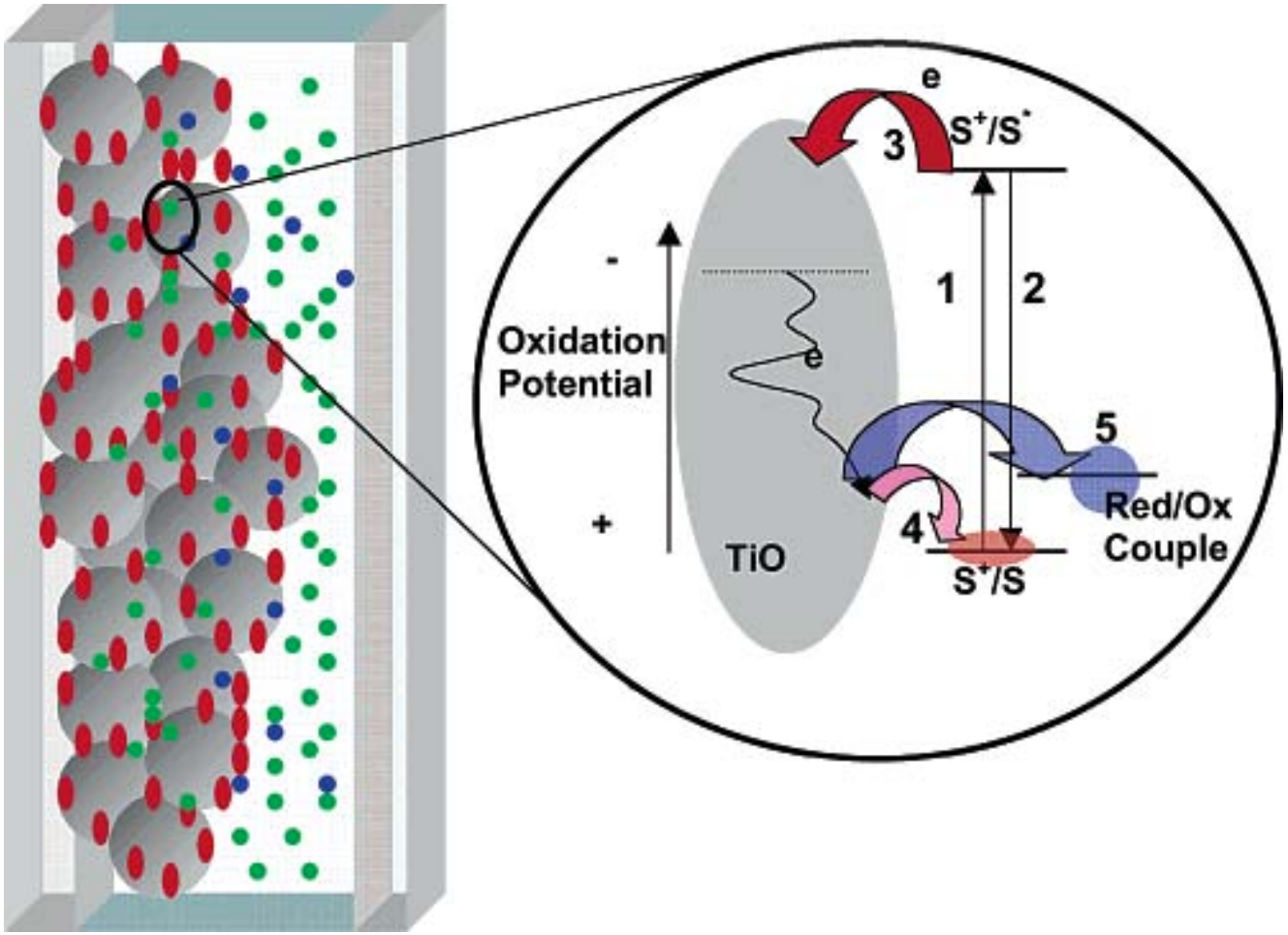

Long Diffusion Distances are Necessary

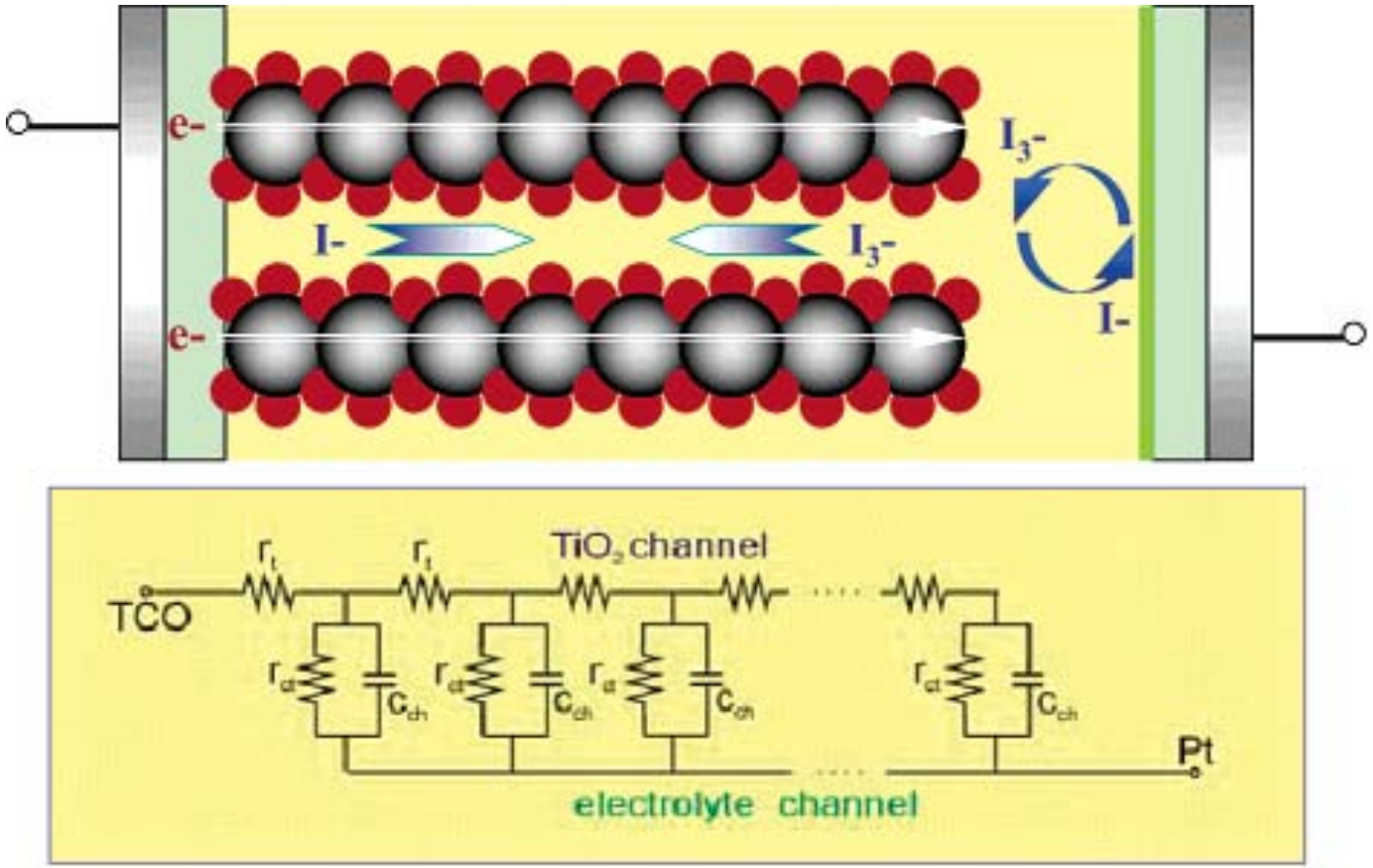

1. FTO/TiO2 interface; 2. TiO2/electrolyte interface; 3. Electrolyte/Pt interface.

TiO_2 Nanoparticle Paste Preparation

Mix 37 ml of Ti-(O*i*-Pr)$_4$ and 10 ml of *i*-PrOH in an addition funnel

▼

Add the mixture to glacial acetic acid (250ml) + H_2O (80 ml) pre-cooled to 0 °C

▼

Stir the solution at 80 °C for 8 hrs

▼

Sonicate in a cell disrupter

▼

Autoclave for 8 hrs at 230 °C

▼

Sonicate in a cell disrupter

▼

Concentrate the paste to 150 g/L or 12 wt % with respect to weight of TiO_2

▼

Add hydroxypropyl cellulose to 6 % wt., stir vigorously for 24 hrs

Zaban, A. *et. al. J. Phys. Chem. B* **1997**, *101*, 55-57

Characterization of TiO_2 Nanoparticles

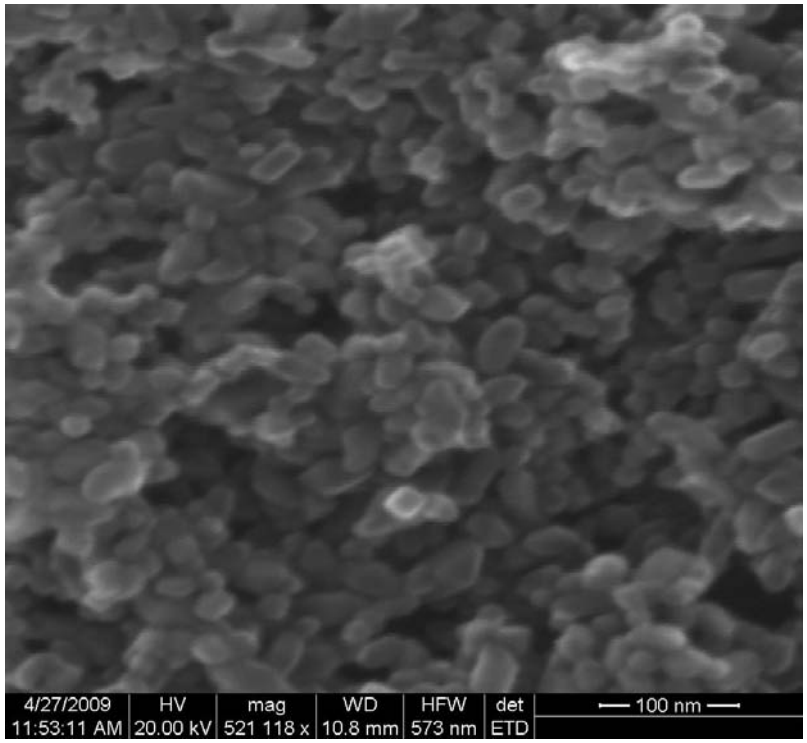

SEM image of TiO_2 nanoparticles

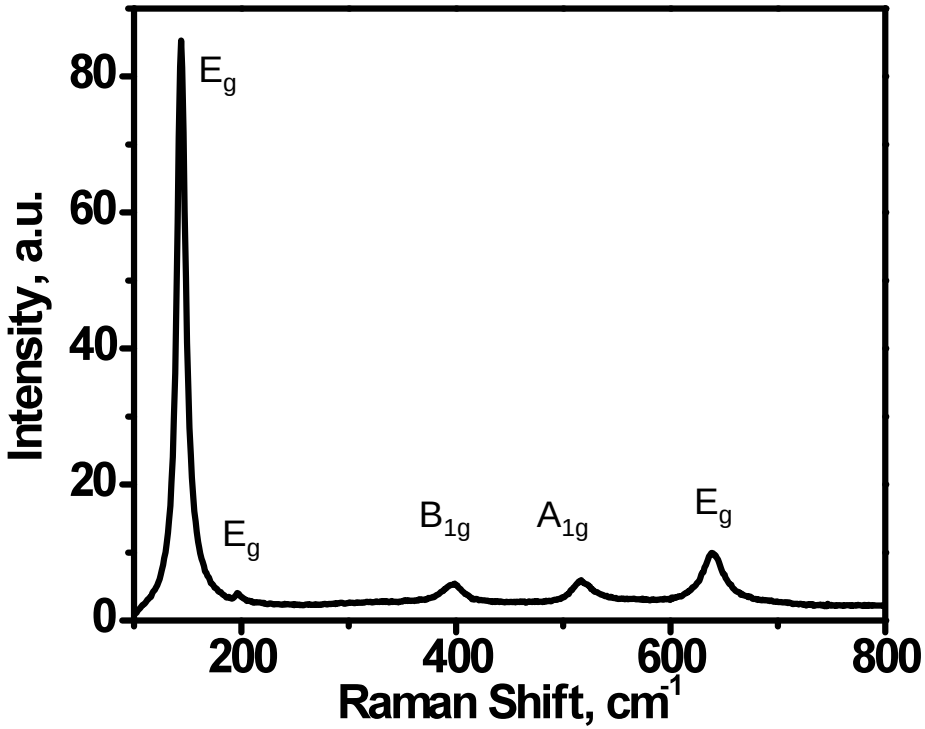

Raman spectrum of TiO_2 film, excitation at 785 nm

Choi, H. C. *et. al. Vibrational Spectroscopy* **1997**, *37*, 33-38

Structure/Function Considerations in Sensitizer Design

- Strong light absorption over a broad spectral range extending into the near-IR
- Proper alignment of molecular energy levels to ensure regenerative behavior
- Metal oxide surface anchoring moiety (such as COOH)
- Long term photochemical stability
- Long term thermal stability
- Compatible with polymer gel electrolytes
- High throughput chemical synthesis (microwave assisted chemistry desirable)
- Color tunable molecules for niche applications

Various Redox Electrolyte Components

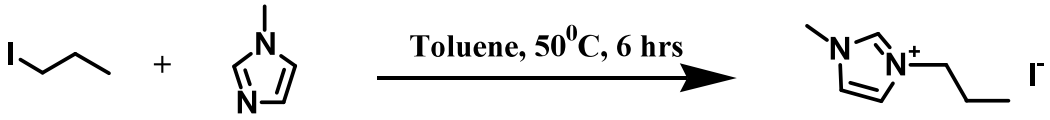

1-methyl-3-propylimidazolium iodide (PMII)
(iodide source, dye regeneration, increases V_{OC})

Tetrahedron **2003**, ***59,*** 2253-2258; *J. Org. Chem.* **2002**, *67,* 3145-3148

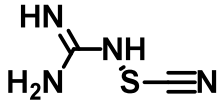

guanidine thiocyanate
(NCS ligand source, dye repair?)

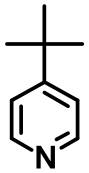

4-*tert*-butylpyridine
(tunes CB potential to more negative potentials, increases V_{OC})

LiI

(tunes CB potential to more positive potentials (Li^+), decreases V_{OC}, iodide source, dye regeneration)

I_2
(iodine source, dye regeneration)

1. Kroeze J. E. *et. al. J. Am. Chem. Soc*. **2006**, *128*, 16376-16383
2. Cameron P. J. *et. al. J. Phys. Chem. B* **2005**, *109*, 930-936
3. Zhang Z. *et. al. Adv. Funct. Mater.* **2008**, *18*, 341-346

Influence of Electrolyte Composition on Density of CB/Trap States in TiO_2

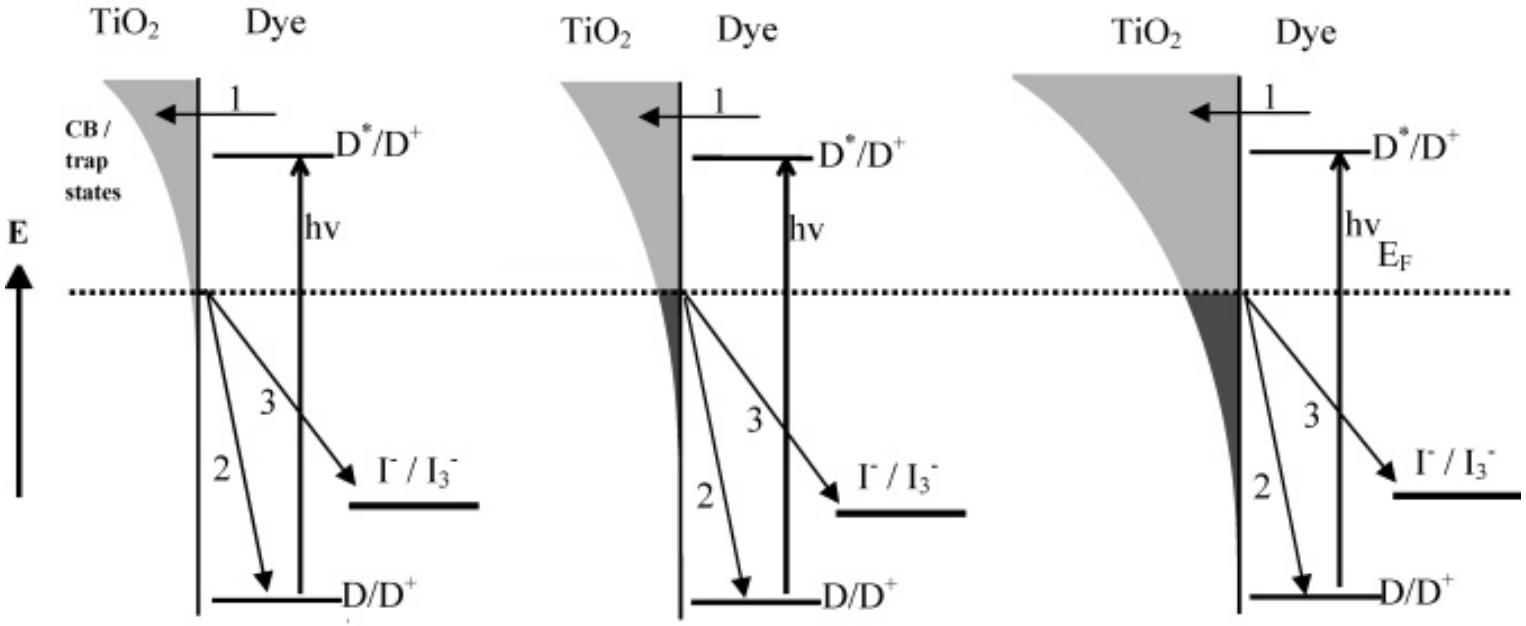

Electrolyte B:
No Li^+

- Slow Electron Injection (1)
- Slow Charge Recombination rates (2) & (3)

Electrolyte A:
Both Li^+ and 4-tert-butyl pyridine

- Intermediate Electron Injection rate (1)
- Intermediate Charge Recombination rates (2) & (3)

Electrolyte C:
No 4-tert-butyl pyridine

- Fast Electron Injection rate (1)
- Fast Charge Recombination rates (2) & (3)

Durrant J. R. *et. al. J. Am. Chem. Soc.* **2005**, *127*, 3456 - 3462

Dynamic Competition

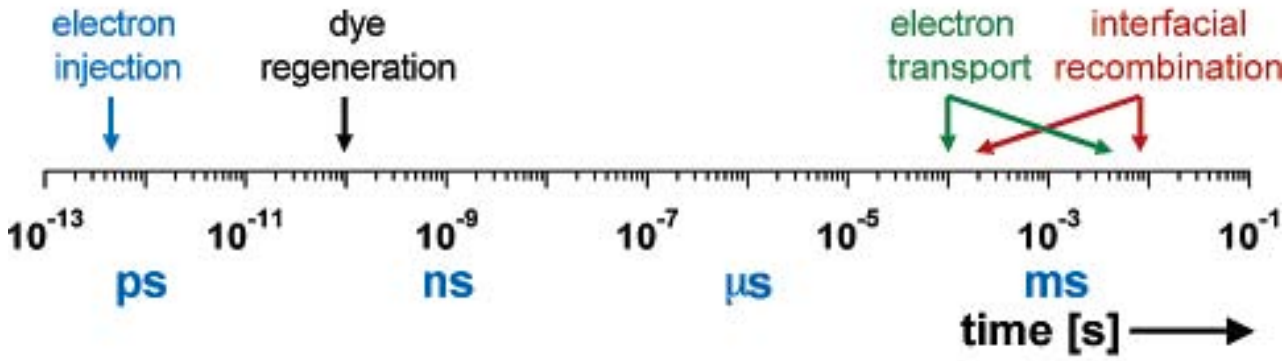

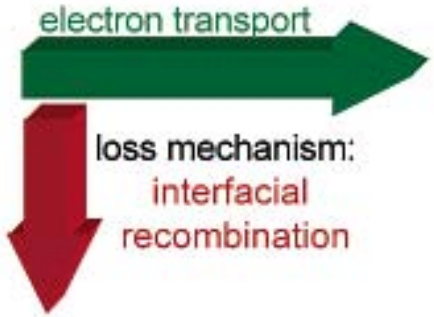

Competition ⇒

Electron diffusion length

$$L_n = \sqrt{D_n \cdot \tau_n}$$

τ_n: electron lifetime

D_n: electron diffusion coefficient

Ultrafast Injection Kinetics

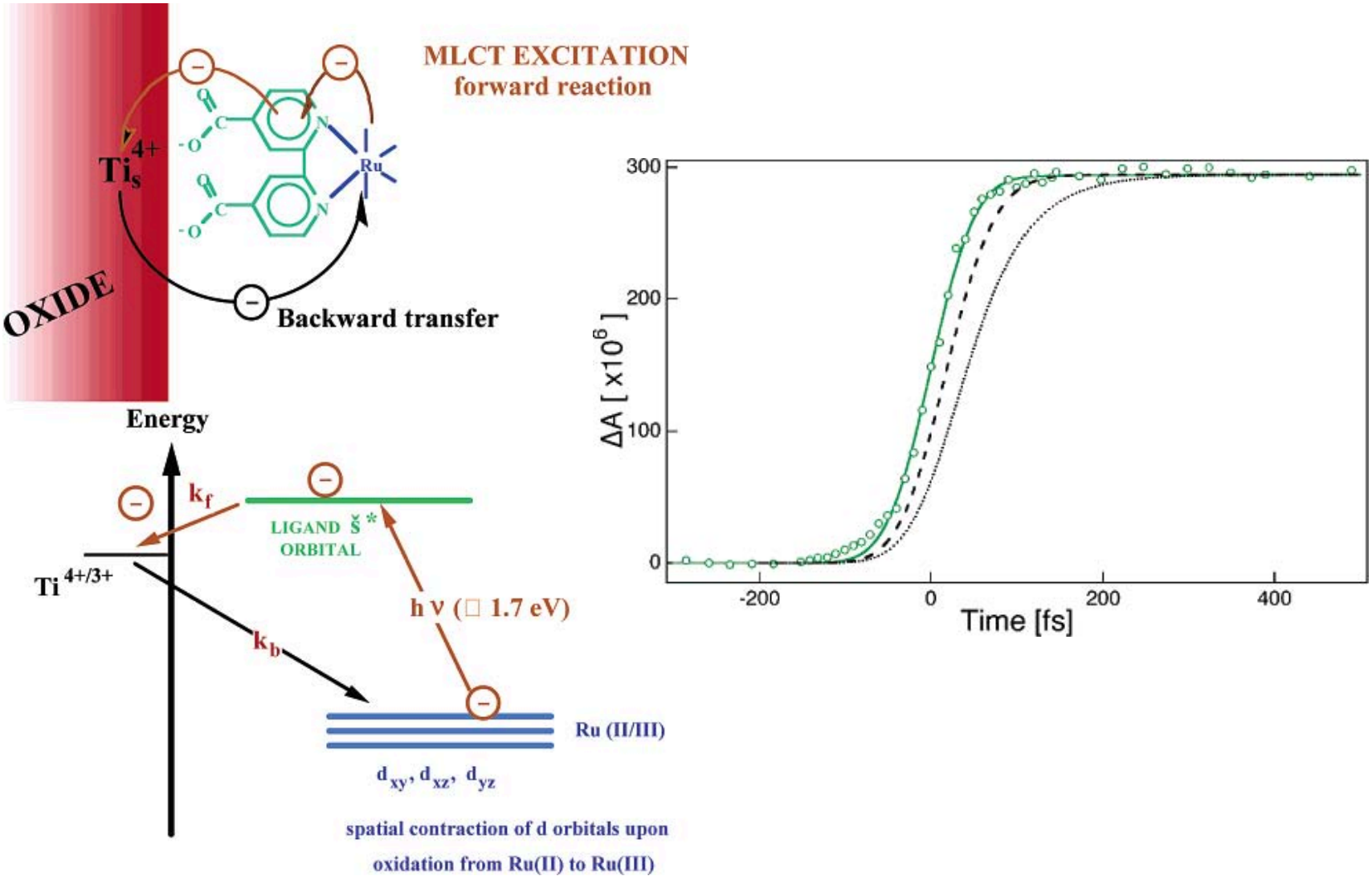

Operational DSSCs

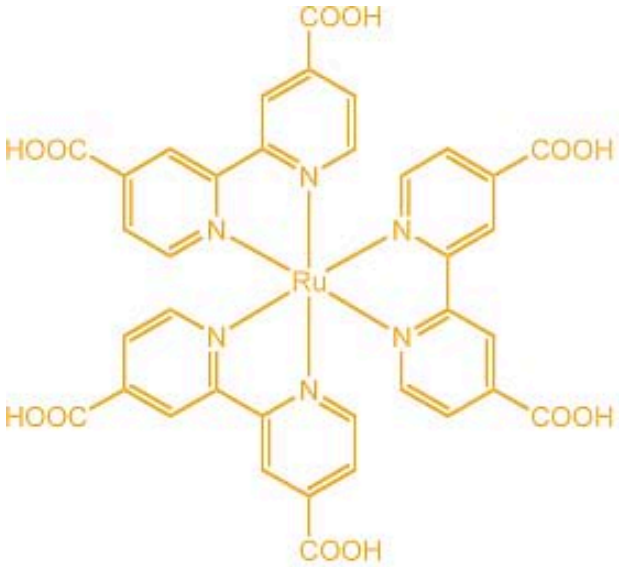

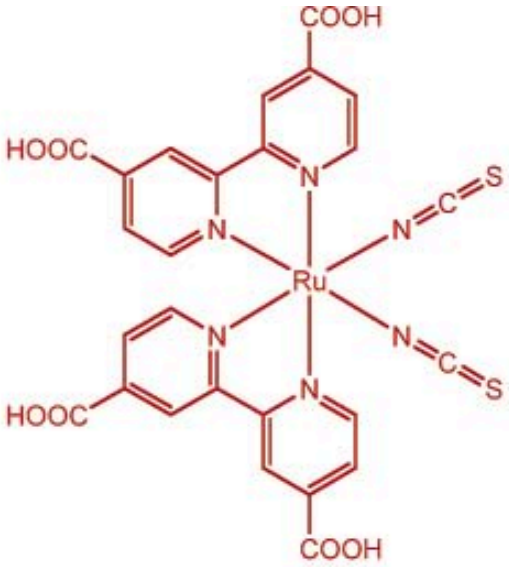

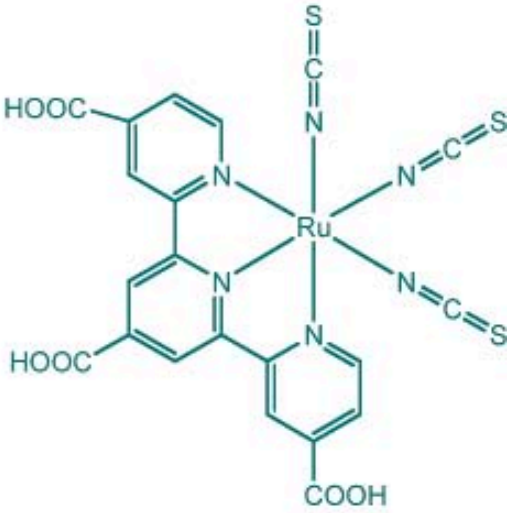

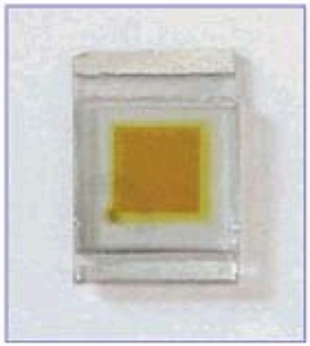

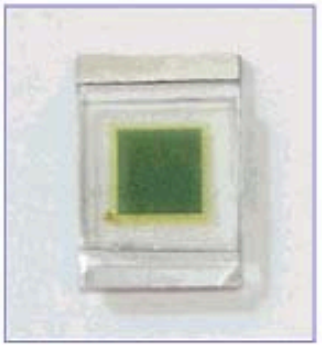

State-of-the-Art Mesoscopic Dye-Sensitized Solar Cells

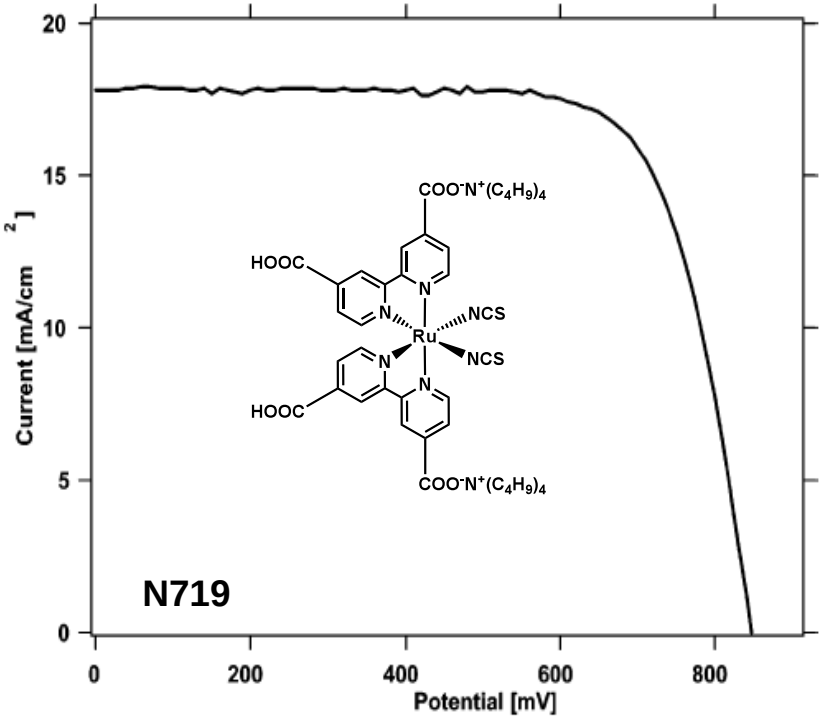

J_{SC} = 17.73 mA/cm^2
V_{OC} = 846 mV
FF = 0.745
Efficiency = 11.18 %

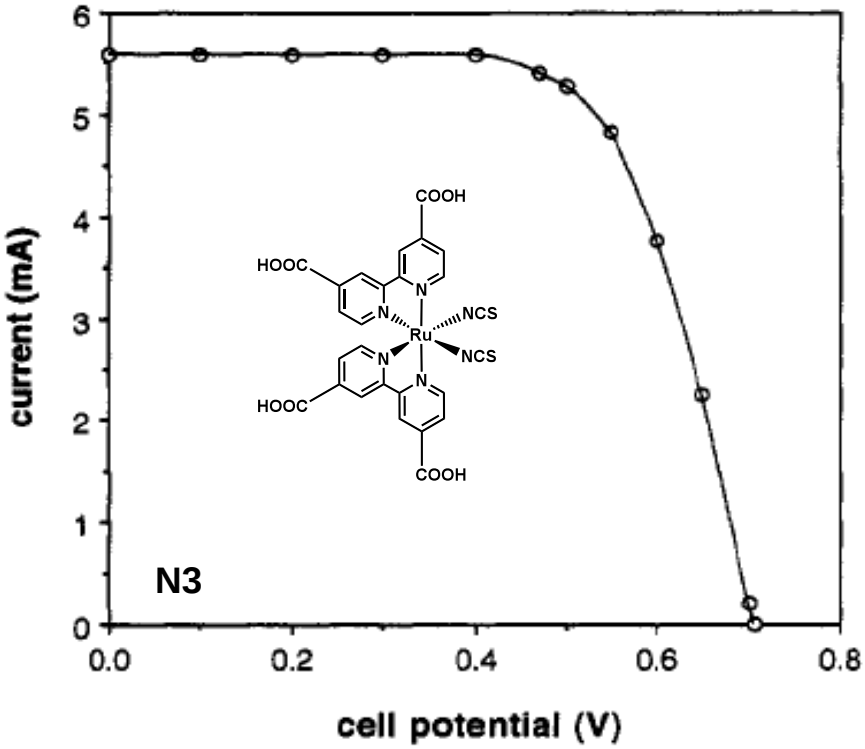

J_{SC} = 18.2 mA/cm^2
V_{OC} = 720 mV
FF = 0.730
Efficiency = 10.00 %

Nazeeruddin M. K. *et. al. J. Am. Chem. Soc.* **1993**, *115*, 6382-6390
Nazeeruddin M. K . *et. al. J. Am. Chem. Soc.* **2005**, *127*, 16835-16847

Photoaction – Single Crystal TiO_2 vs. Mesoscopic TiO_2

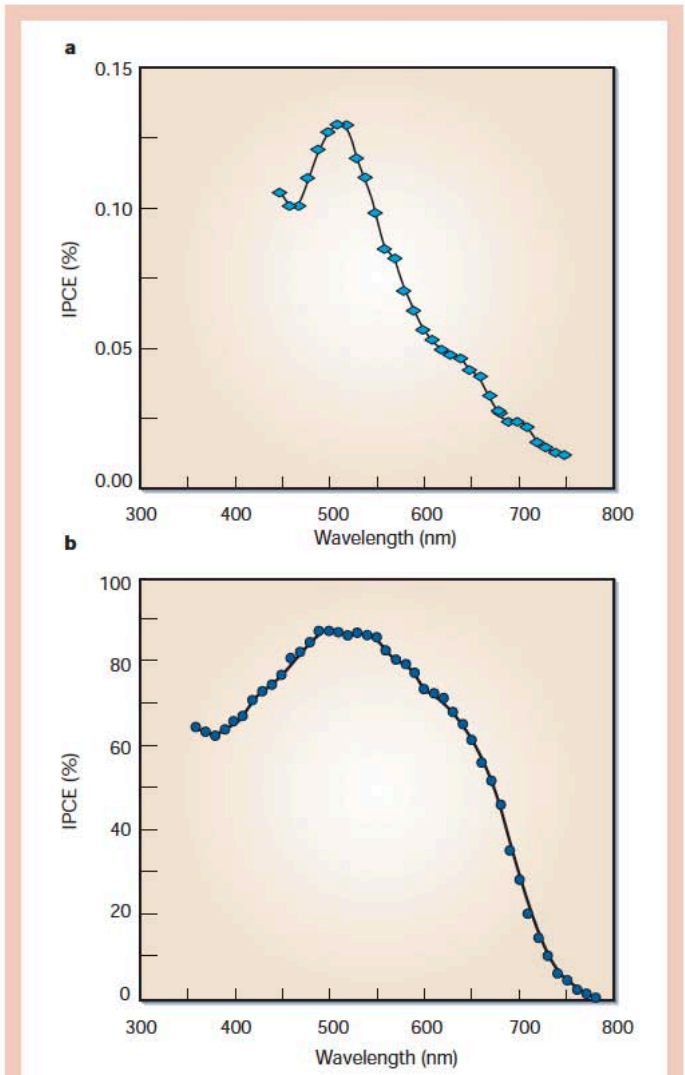

Figure 5 The nanocrystalline effect in dye-sensitized solar cells. In both cases, TiO_2 electrodes are sensitized by the surface-anchored ruthenium complex *cis*-$RuL_2(SCN)_2$. The incident-photon-to-current conversion efficiency is plotted as a

Present DSSC Efficiency Record

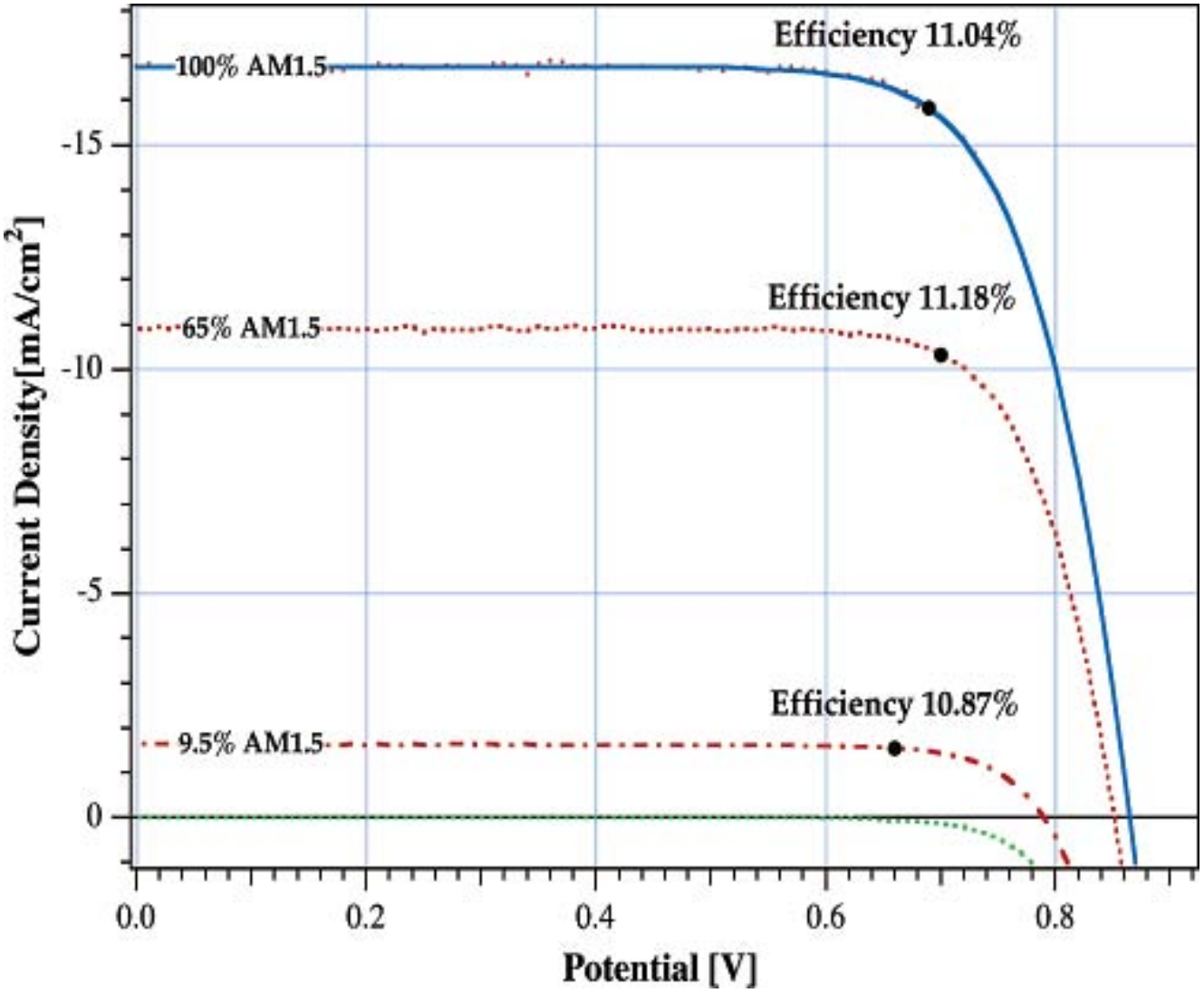

Our Best Operational Devices To Date

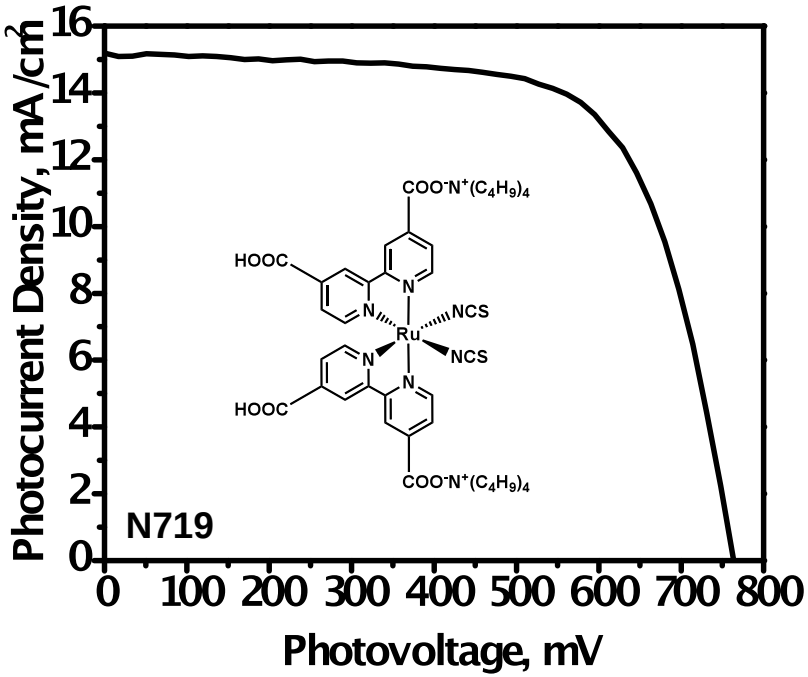

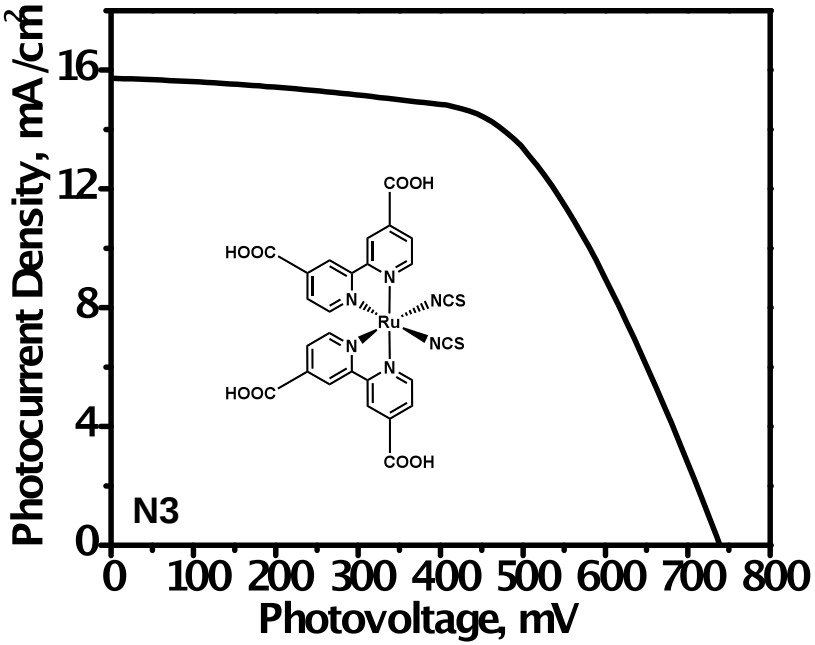

J_{SC} = 15.2 mA/cm^2
V_{OC} = 763 mV
FF = 69 %
Efficiency = 8.0 %

J_{SC} = 15.7 mA/cm^2
V_{OC} = 739 mV
FF = 58 %
Efficiency = 6.7 %

Electrolyte: 0.1 M LiI, 0.05 M I_2, 0.6 M 1-methyl-3-*n*-propylimidazolium iodide, 0.1 M guanidine thiocyanate, 0.5 M 4-*tert*butyl-pyridine in CH_3CN. LiI concentration was varied as shown
Device active area: 0.25 cm^2. Films sintered at 500 °C for 30 min., sensitized 48 hrs.
TiO_2 film thickness: 12 μm. Transparent paste only. No $TiCl_4$ treatment!

Solar Fuels Integration – Tandem Cells for Water Splitting

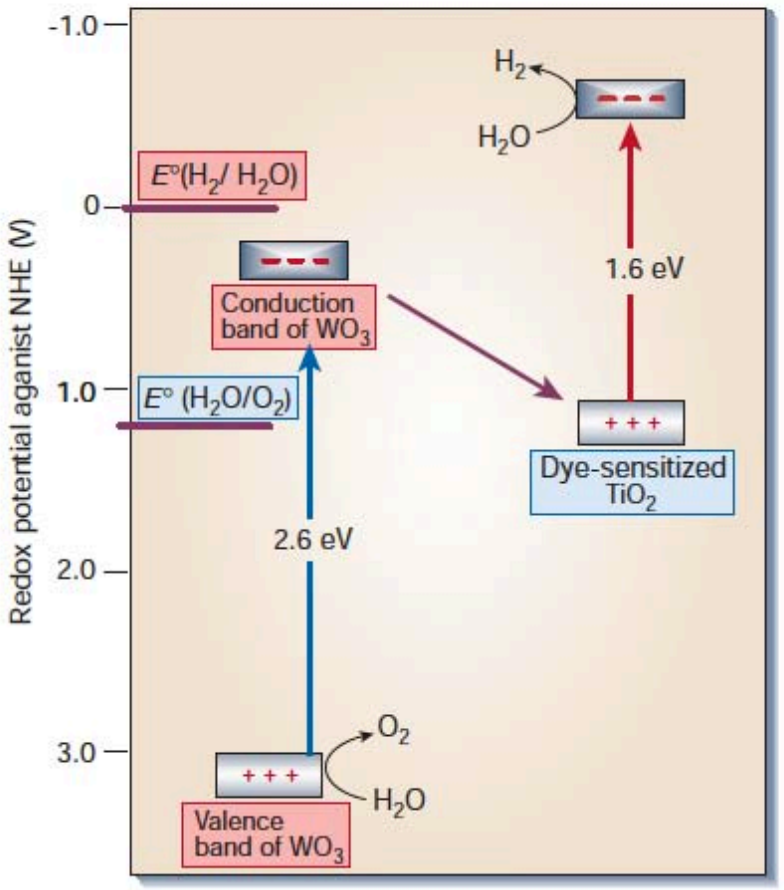

Figure 6 The Z-scheme of photocatalytic water decomposition by a tandem cell.

Semiconductor Material Selection

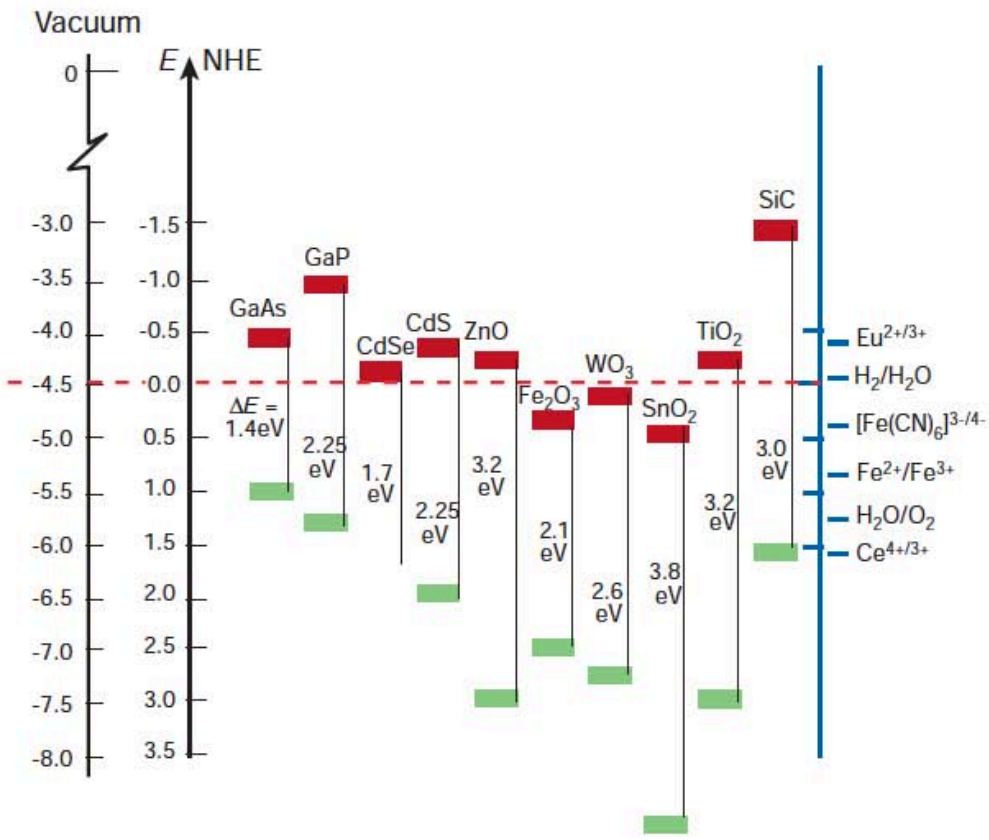

Figure 2 Band positions of several semiconductors in contact with aqueous electrolyte at pH 1. The lower edge of the conduction band (red colour) and upper edge of the valence band (green colour) are presented along with the band gap in electron volts. The energy scale is indicated in electron volts using either the normal hydrogen electrode (NHE) or the vacuum level as a reference. Note that the ordinate presents internal and not free energy. The free energy of an electron–hole pair is smaller than the band gap energy due to the translational entropy of the electrons and holes in the conduction and valence band, respectively. On the right side the standard potentials of several redox couples are presented against the standard hydrogen electrode potential.

TiO_2 Nanotube-based DSSCs: Current State

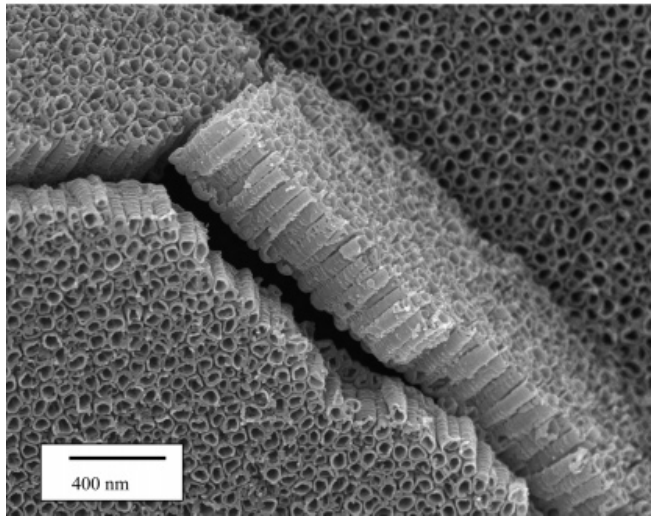

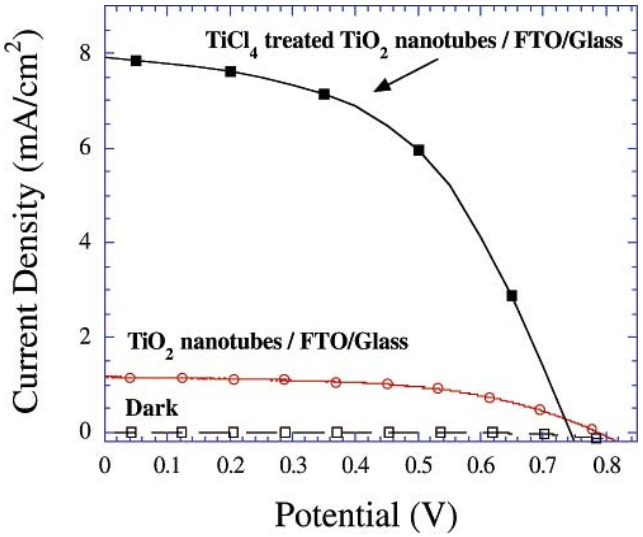

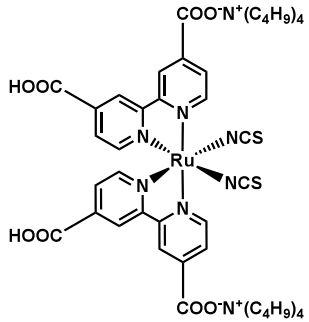

Dye: N719
J_{SC} = 7.87 mA/cm^2
V_{OC} = 750 mV
FF = 0.490
Efficiency = 2.90 %

Gopal, K. M. *et. al. NanoLetters* **2006**, *6,* 215-218

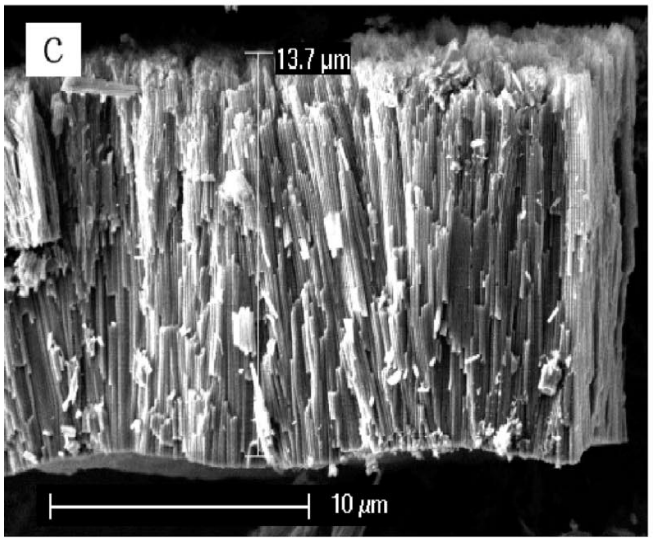

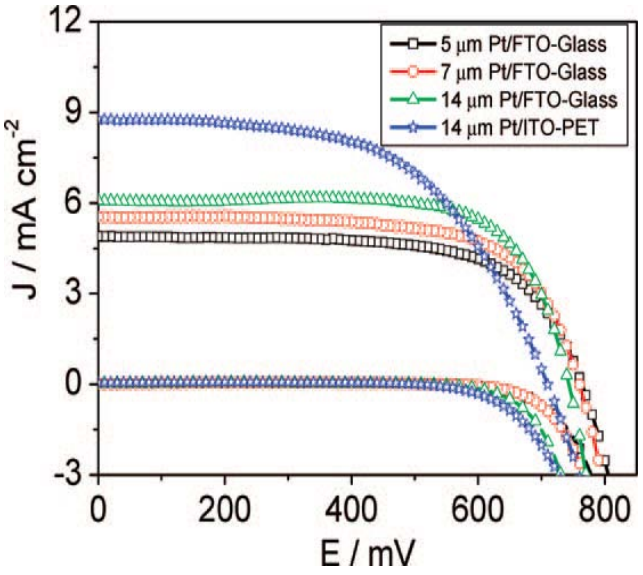

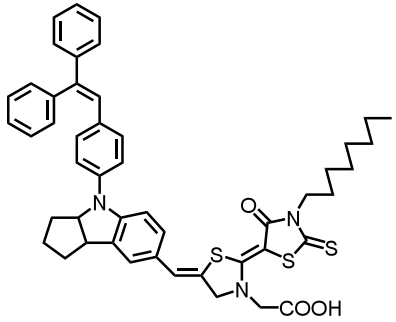

Dye: D205
J_{SC} = 8.99 mA/cm^2
V_{OC} = 709 mV
FF = 0.561
Efficiency = 3.58 %

Kuang, D. *et. al. ACS Nano* **2008**, *2,* 1113-1116

Jablonski Diagram for Os^{II} MLCT Complexes

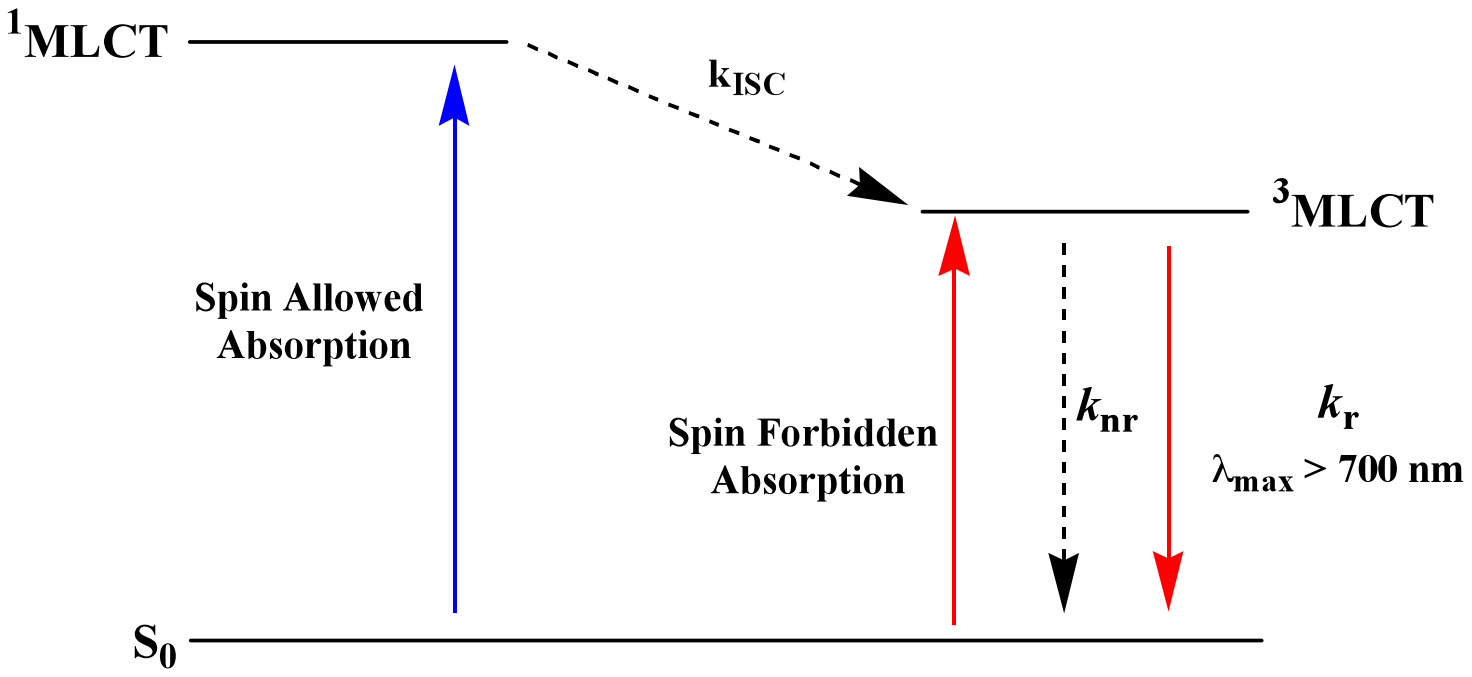

Can the $S_0 \rightarrow T_1$ transition be manipulated with variation in π-conjugation in the imine ligand?

Advantages of Os^{II} over Ru^{II}

- Larger value of Δ_o, which leads to higher energies for d-d (MC) excited states (no thermal activation)
- Greater extension of the metal *d*-orbitals which can enhance metal - ligand σ-bonding (and π-backbonding)
- Large value of the spin-orbit coupling constant greatly relaxes spin selection rules
- Red to near-IR absorption profiles
- Os^{II} MLCT complexes more photochemically/thermally stable relative to those based on Ru^{II}

1. Kober, E. M. *et. al. Inorg. Chem.* **1988**, *27*, 4587-4598
2. Kalyanasundaram, K. *Photochemistry of polypyridine and porphyrin complexes*; San Diego: California, **1992**.

Synthesis of Os^{II} Dyes of Mixed Denticity

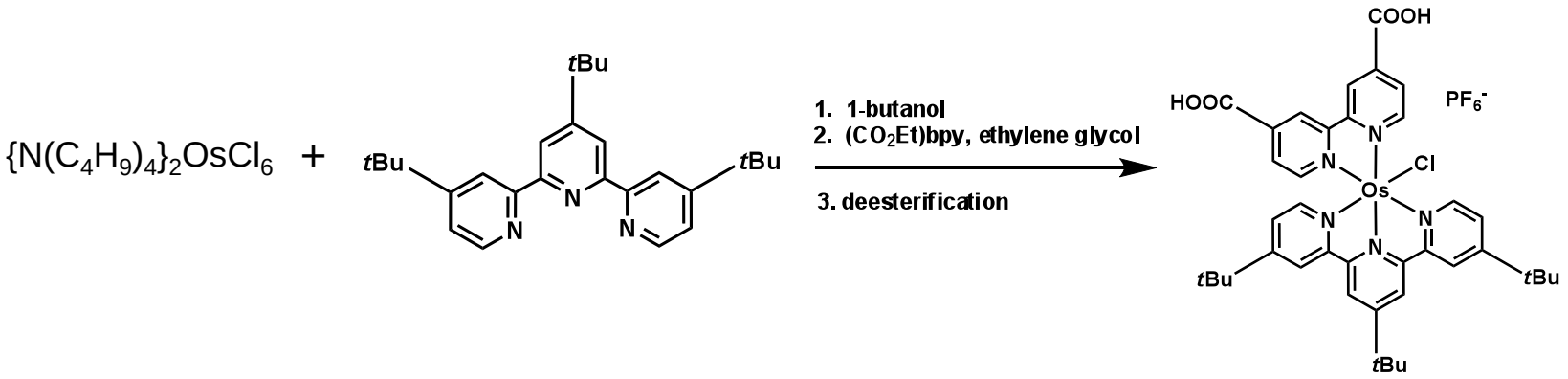

D31

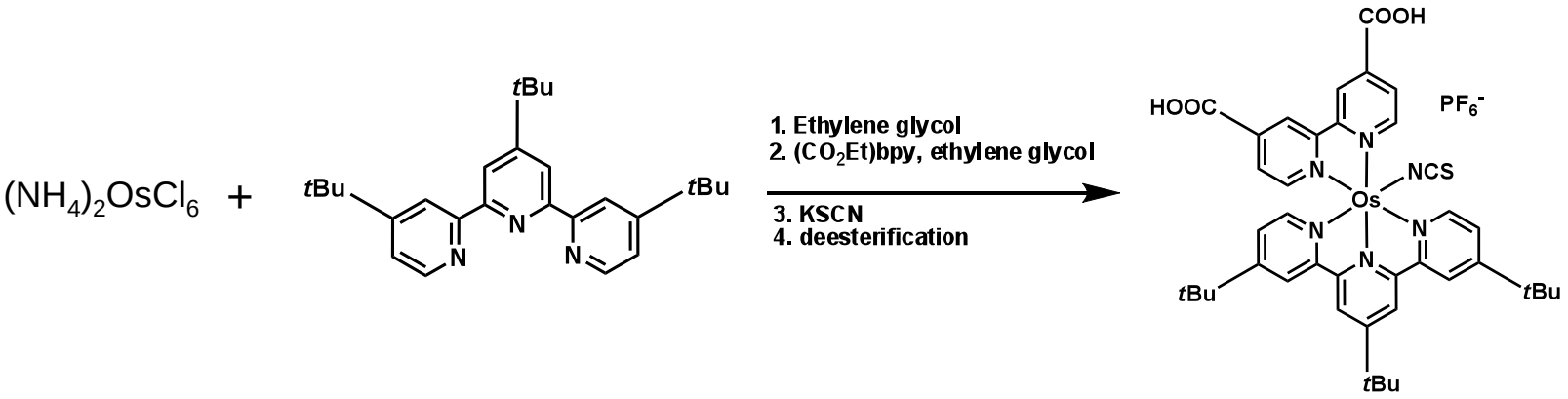

D081

Os^{II} Dyes: Photophysics and Electrochemistry

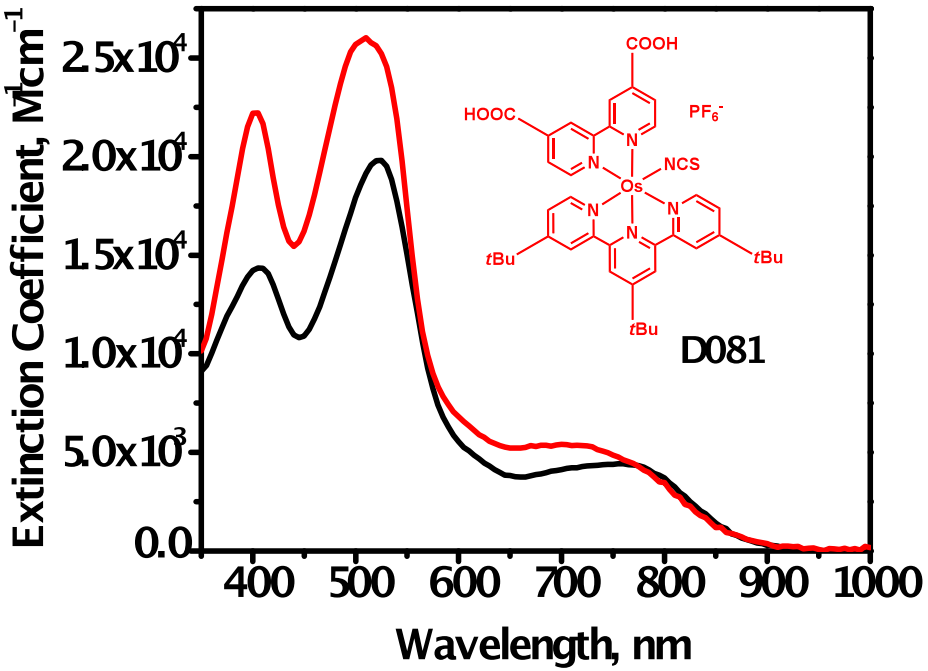

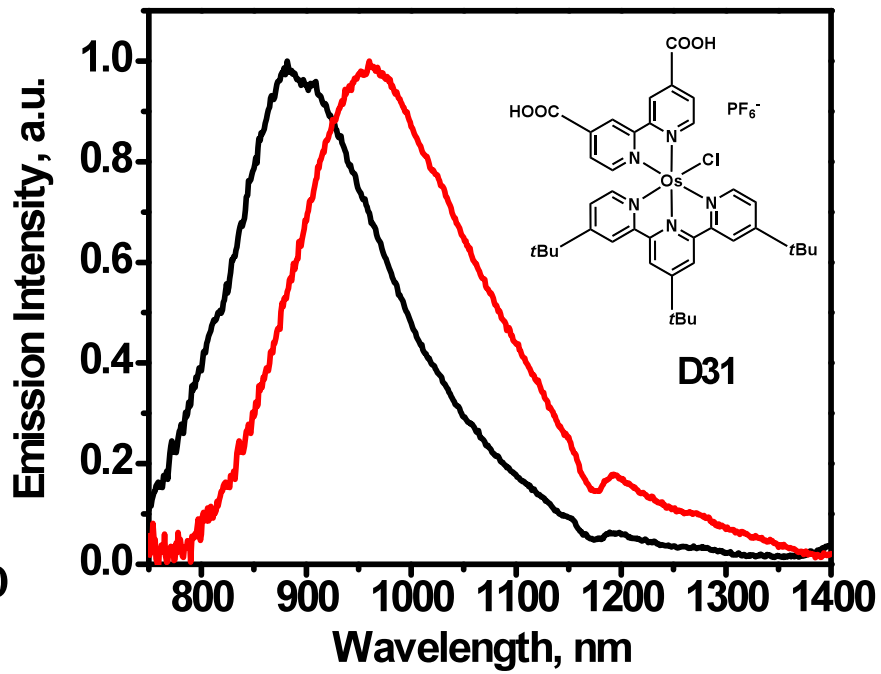

Compound	Absorption max, nm (ε x 10^4, M^{-1} cm^{-1})	Emission max, nm	$E_{1/2}$, V vs NHE[a]
D31	405 (1.44), 525 (1.98), 760 (0.44)	890	0.74[b]
D081	405 (2.22), 510 (2.60), 700 (0.54)	960	0.88
N3[c]	313 (3.12), 396 (1.40), 534 (1.42)	755	1.09
I^-/I_3^-			0.4[d]

[a] In CH_3CN solution with 0.1 M TBA(PF_6) as supporting electrolyte and determined by CV; [b] Determined by DPV; [c] taken from *J. Am. Chem. Soc.* **1993**, *115*, 6382 – 6390; [d] taken from *Adv. Funct. Mater.* **2008**, *18,* 341 – 346.

Os^{II} Dyes: Photovoltaic Performance

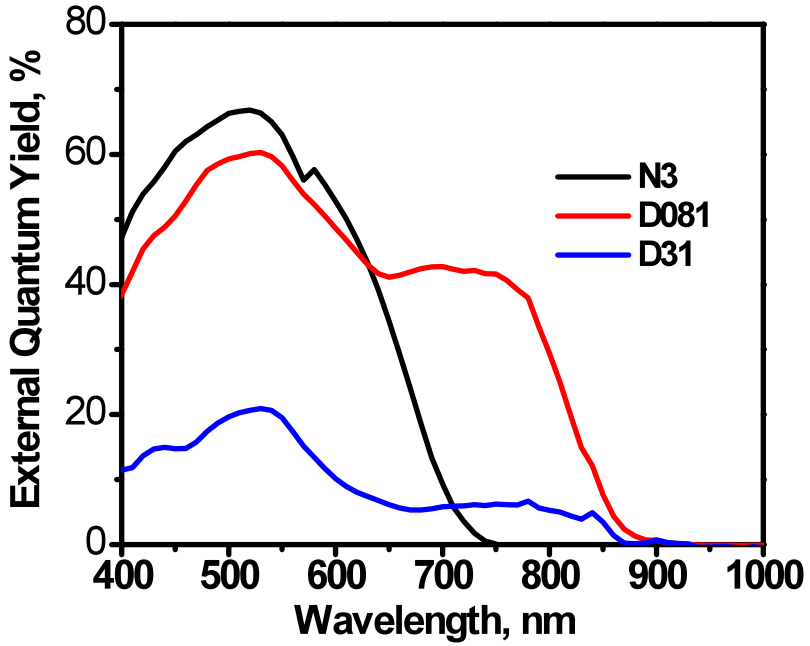

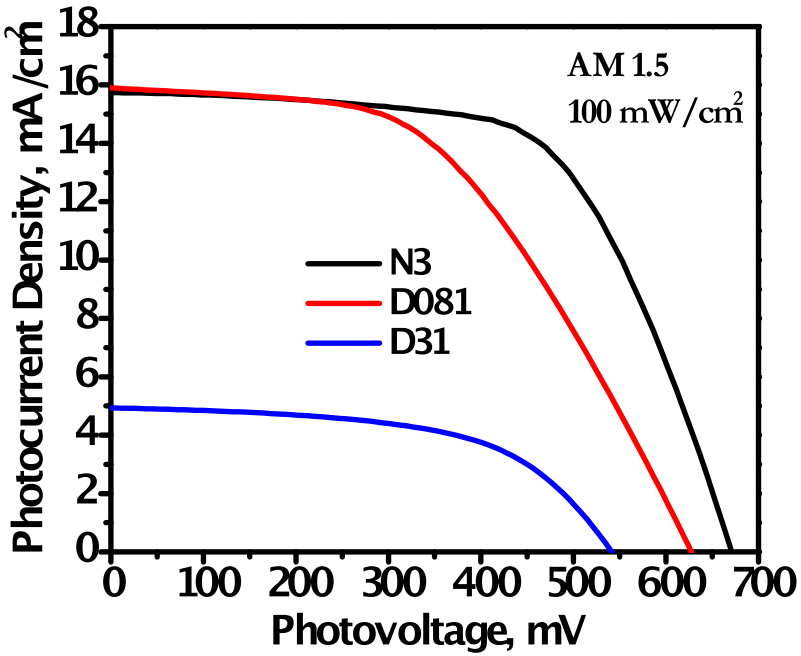

::

Parameter	N3	D081	D31
J_{sc}, mA/cm²	15.7	15.9	4.94
V_{oc}, mV	671	627	542
FF, %	61.7	49.5	56.2
η, %	6.52	4.94	1.50

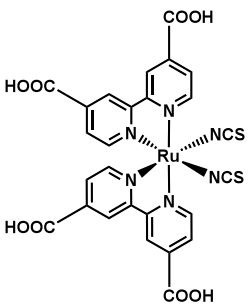

N3

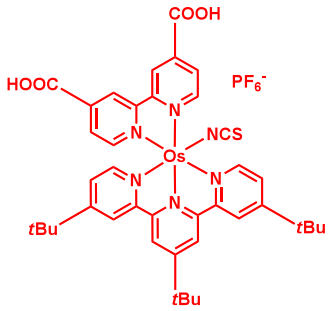

D081

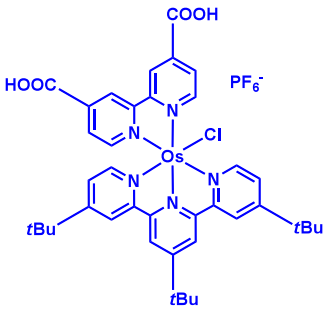

D31

Electrolyte: 0.1 M LiI, 0.05 M I_2, 0.6 M 1-methyl-3-*n*-propylimidazolium iodide, 0.1 M guanidine thiocyanate, 0.5 M 4-*tert*-butylpyridine in CH_3CN

Device active area: 0.16 cm^2 (N3), 0.25 cm^2 (D081/D31), TiO_2 film thickness: 12 μm. Transparent paste only. No $TiCl_4$ for N3; D081/D31 - $TiCl_4$ treated. Films sintered at 500°C for 30 min., sensitized 48 hrs.

Influence of Iodide Concentration on the PV Performance of Os^{II}: Dye Regeneration Limited

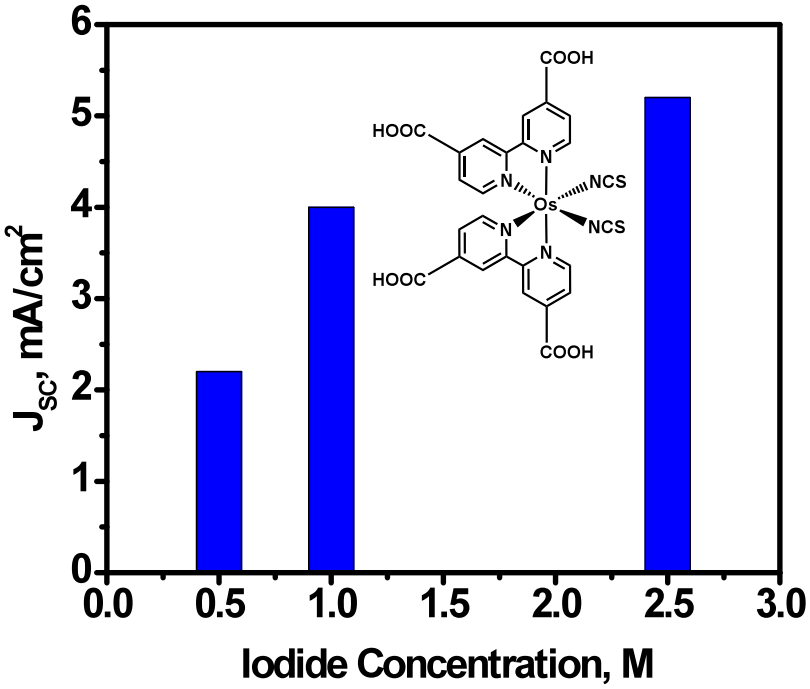

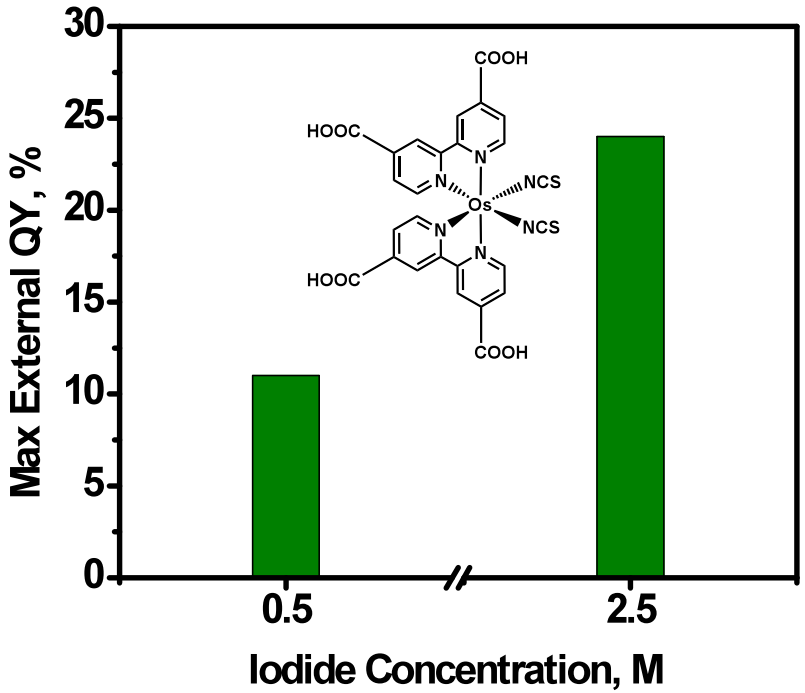

- J_{SC} increased from 2.2 to 5.2 mA/cm^2 upon 5-fold increase in LiI concentration.
- Net effect was attributed to the increase in iodide concentration (LiI + $LiClO_4$).
- However, no significant increase in J_{SC} was observed for corresponding Ru^{II} dyes.

Lewis N. S. *et. al. J. Phys. Chem. B* **2000**, *104*, 6821-6836

Influence of Lithium Iodide Concentration in N3: [Li^+] Lowers CB Edge Decreasing V_{OC}

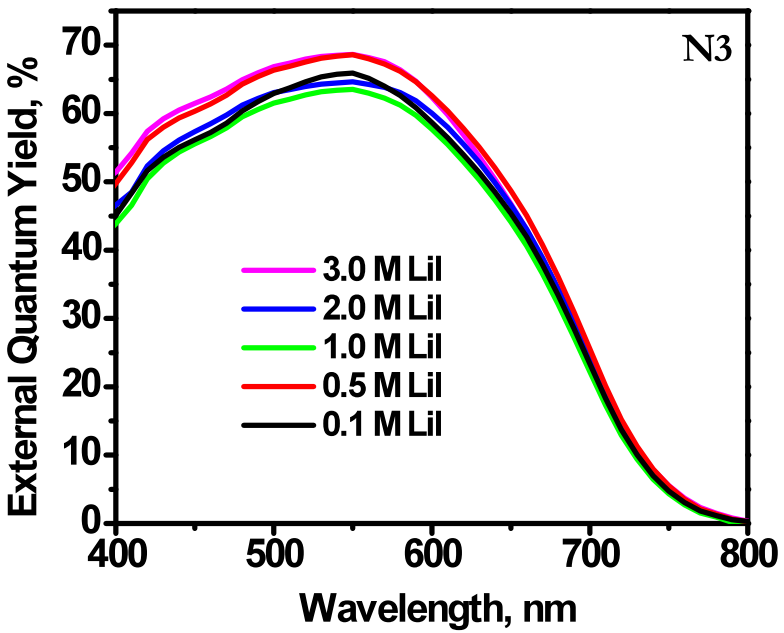

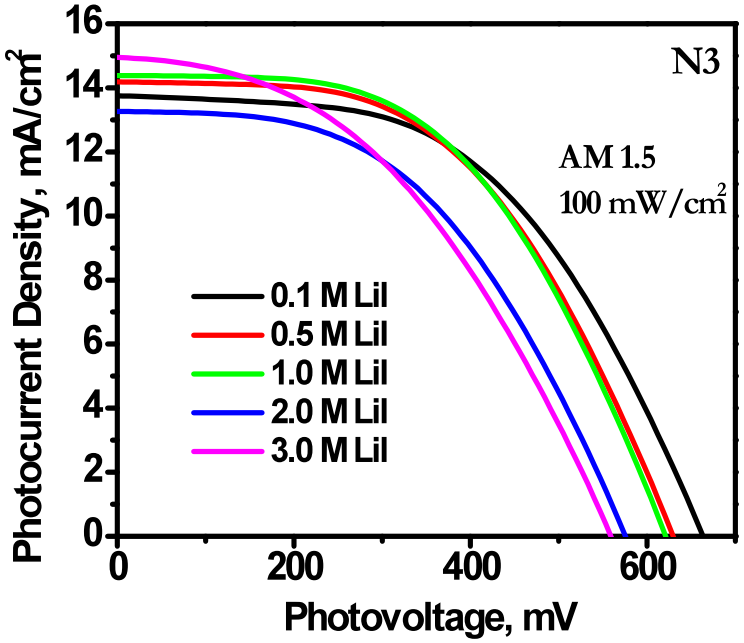

::

N3	0.1 M LiI	0.5 M LiI	1.0 M LiI	2.0 M LiI	3.0 M LiI
J_{sc}, mA/cm²	13.8	14.2	14.4	13.3	15.0
V_{oc}, mV	664	630	621	576	559
FF, %	51.8	51.5	51.7	48.7	42.8
η, %	4.73	4.60	4.61	3.72	3.58

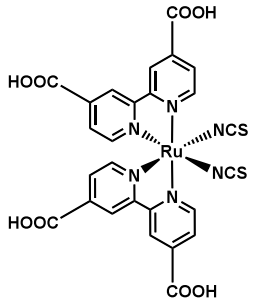

N3

Electrolyte: 0.1 M LiI, 0.05 M I_2, 0.6 M 1-methyl-3-*n*-propylimidazolium iodide, 0.1 M guanidine thiocyanate, 0.5 M 4-*tert*-butylpyridine in CH_3CN. LiI concentration was varied as shown.
Device active area: 0.25 cm^2. $TiCl_4$ treatment for all slides. Films sintered at 500°C for 30 min., sensitized 48 hrs. TiO_2 film thickness: 12 μm. Transparent paste only.

Influence of Lithium Iodide Concentration in D081: A Combination of Both Effects?

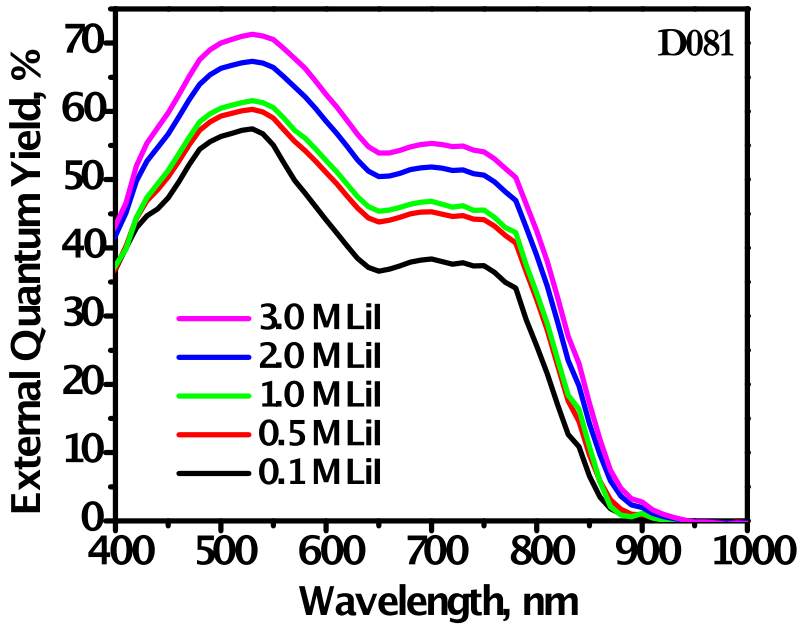

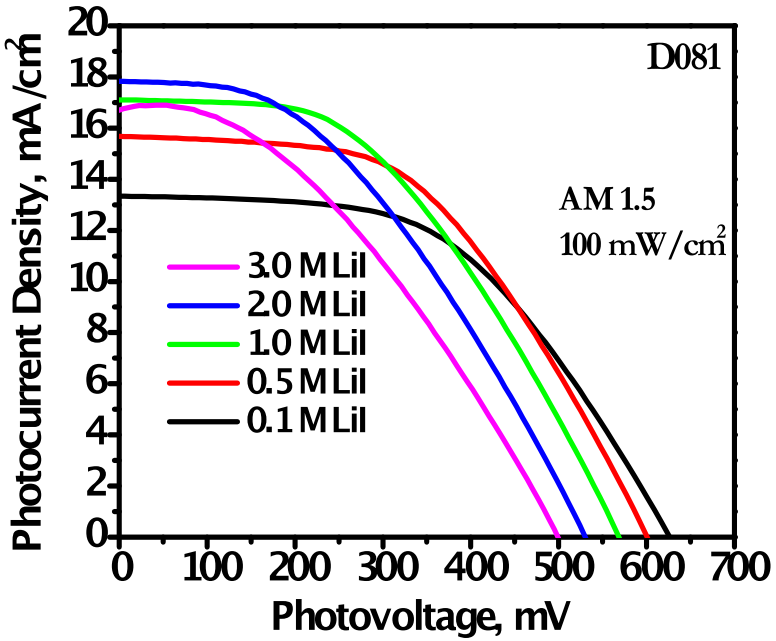

D081	0.1 M LiI	0.5 M LiI	1.0 M LiI	2.0 M LiI	3.0 M LiI
J_{sc}, mA/cm²	13.3	15.7	17.1	17.8	16.7
V_{oc}, mV	626	601	569	530	499
FF, %	52.0	50.1	46.0	41.5	38.9
η, %	4.34	4.72	4.48	3.92	3.24

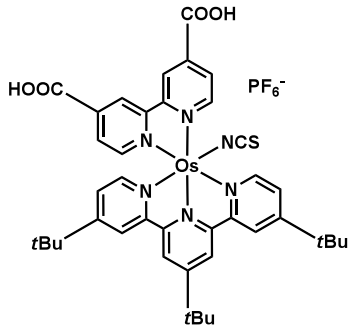

D081

Electrolyte: 0.1 M LiI, 0.05 M I_2, 0.6 M 1-methyl-3-*n*-propylimidazolium iodide, 0.1 M guanidine thiocyanate, 0.5 M 4-*tert*-butylpyridine in CH_3CN. LiI concentration was varied as shown.
Device active area: 0.25 cm². $TiCl_4$ treatment for all slides. Films sintered at 500°C for 30 min., sensitized 48 hrs. TiO_2 film thickness: 12 µm. Transparent paste only.

Questions?

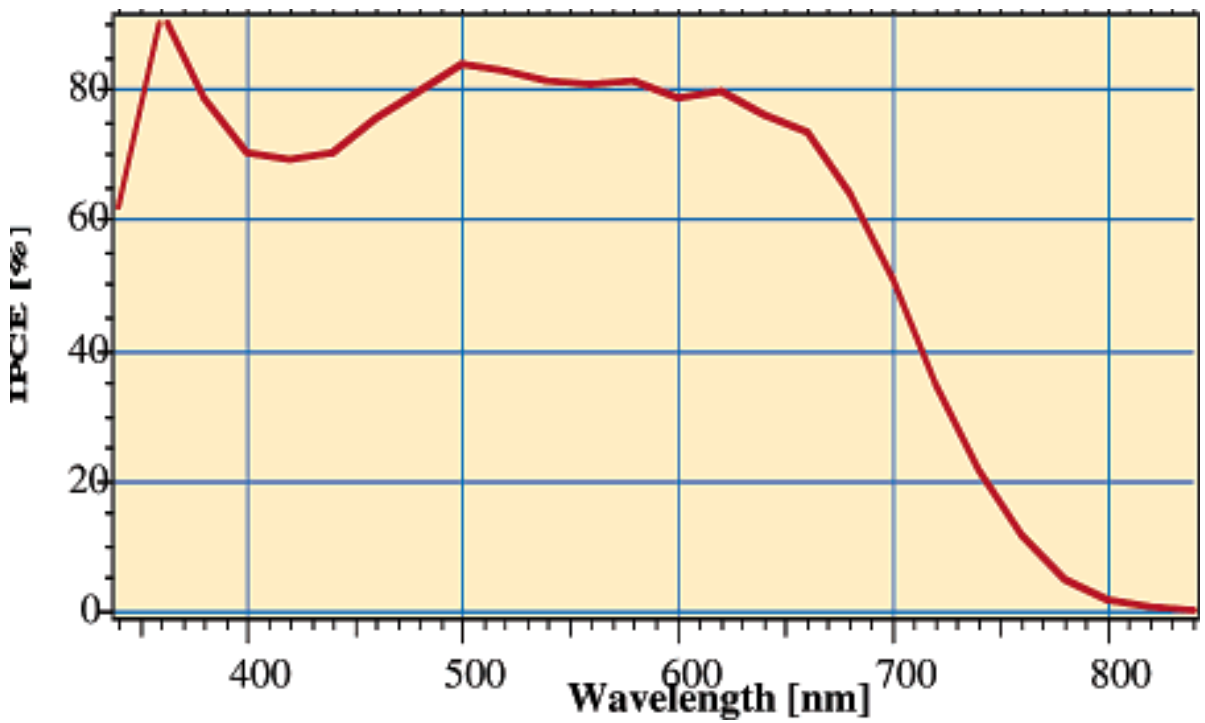
IPCE [%]
80
60
40
20
0
400
500
600
700
800
Wavelength [nm]

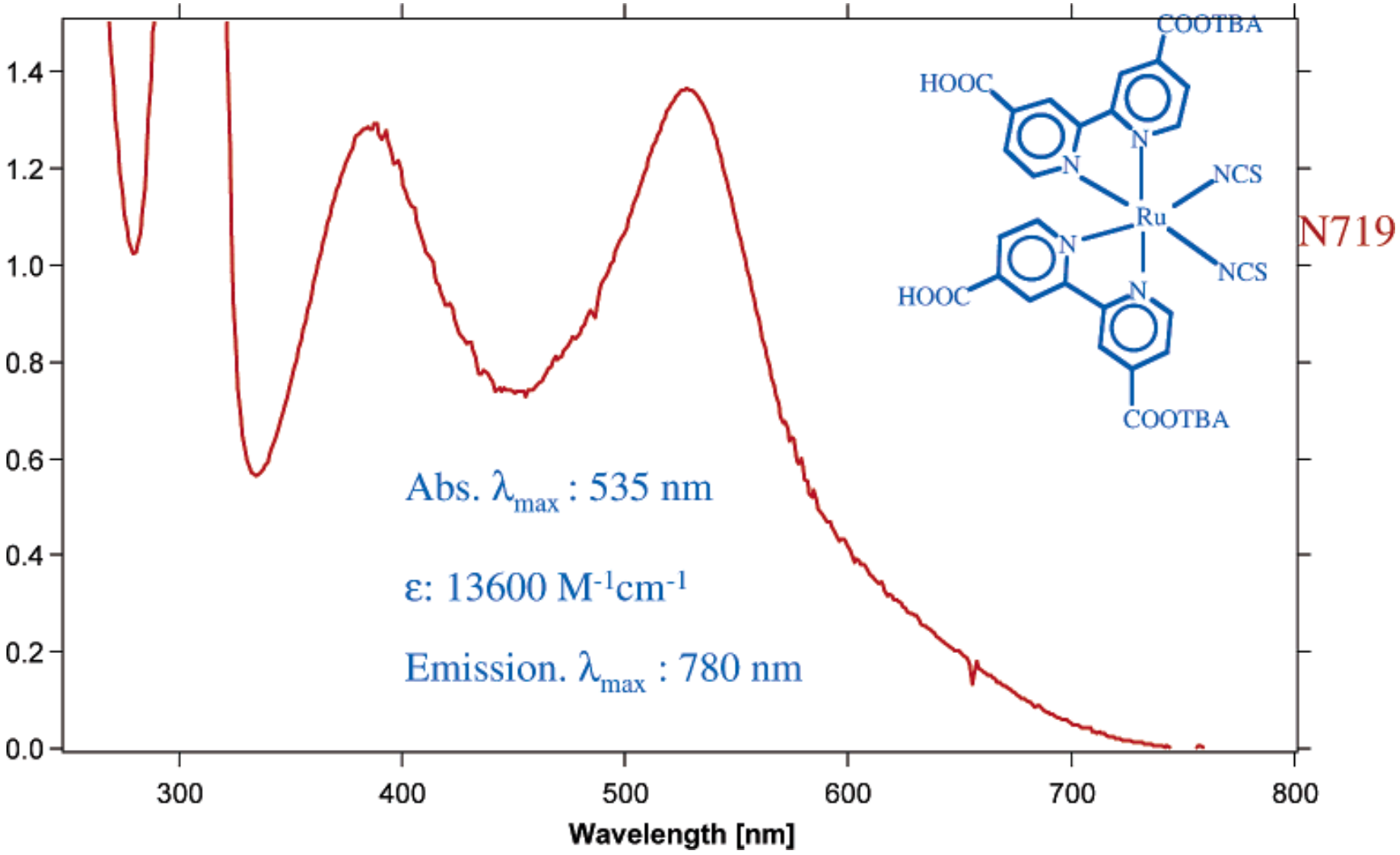
1.4
1.2
1.0
0.8
0.6
0.4
0.2
0.0
300
400
500
600
700
800
Wavelength [nm]
Abs. λmax : 535 nm
ε: 13600 M-1cm-1
Emission. λmax : 780 nm
COOTBA
HOOC
N
N
NCS
Ru
N
NCS
HOOC
N
COOTBA
N719

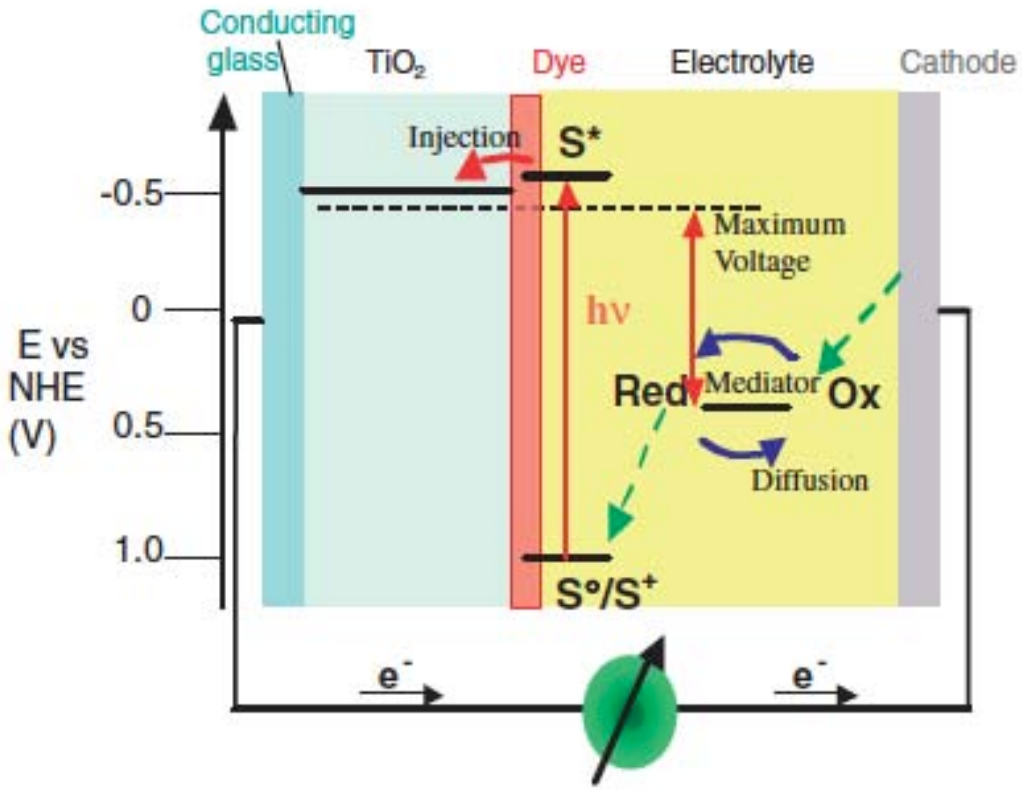
Conducting glass
TiO2
Dye
Electrolyte
Cathode
Injection
S*
-0.5
0
0.5
1.0
E vs NHE (V)
Maximum Voltage
hν
Red
Mediator
Ox
Diffusion
S°/S+
e-
e-

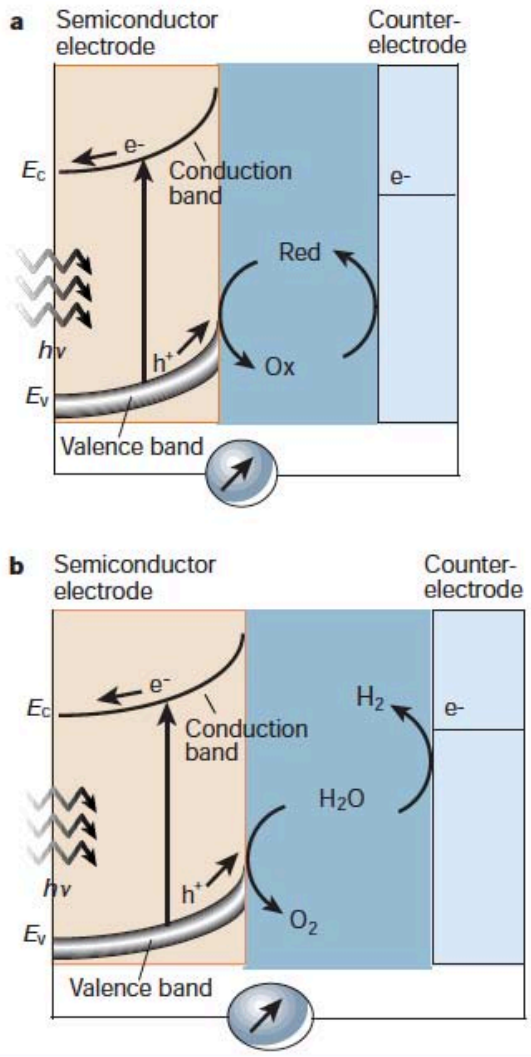

Figure 1 Principle of operation of photoelectrochemical cells based on *n*-type semiconductors. **a**, Regenerative-type cell producing electric current from sunlight; **b**, a cell that generates a chemical fuel, hydrogen, through the photo-cleavage of water.

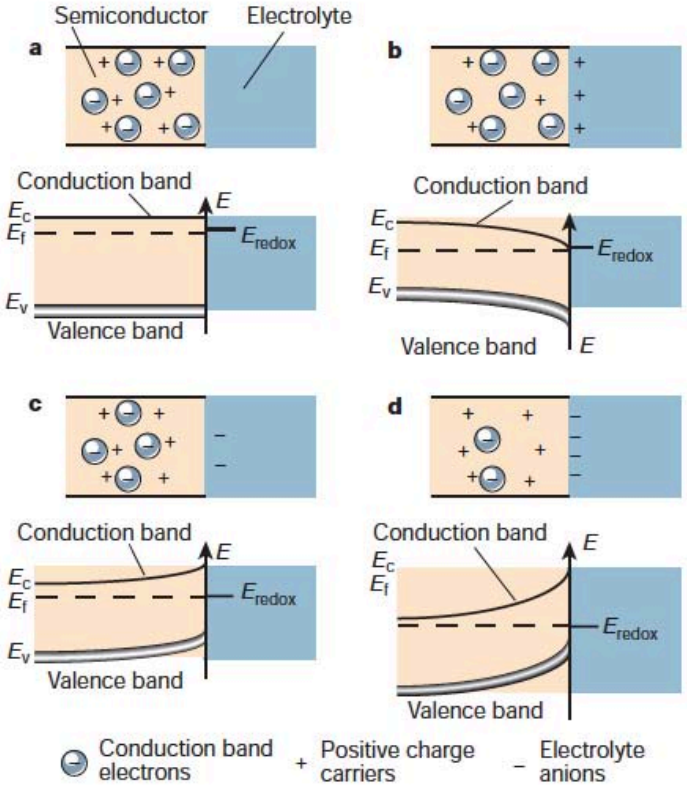

Box 1 Figure Schematic showing the electronic energy levels at the interface between an *n*-type semiconductor and an electrolyte containing a redox couple. The four cases indicated are: **a**, flat band potential, where no space-charge layer exists in the semiconductor; **b**, accumulation layer, where excess electrons have been injected into the solid producing a downward bending of the conduction and valence band towards the interface; **c**, depletion layer, where electrons have moved from the semiconductor to the electrolyte, producing an upward bending of the bands; and **d**, inversion layer where the electrons have been depleted below their intrinsic level, enhancing the upward band bending and rendering the semiconductor *p*-type at the surface.

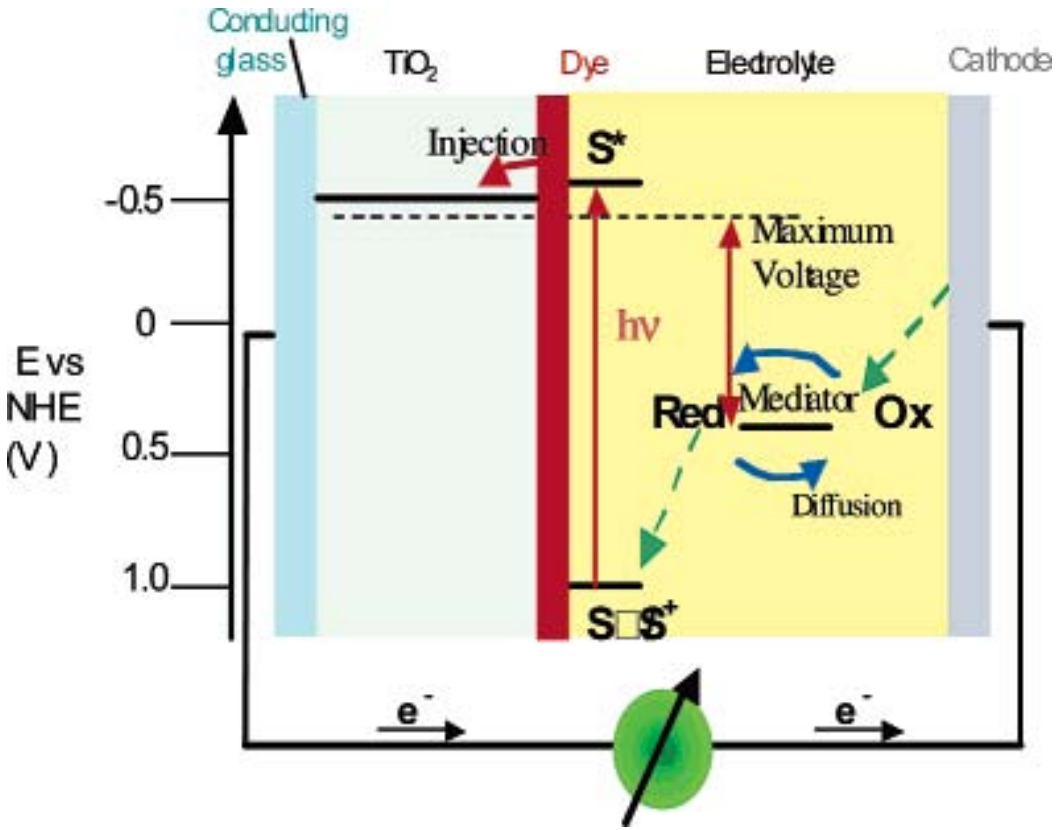
Conducting glass
TiO2
Dye
Electrolyte
Cathode
Injection
S*
-0.5
0
0.5
1.0
E vs NHE (V)
Maximum Voltage
hν
Red
Mediator
Ox
Diffusion
S/S+
e-
e-